FEATURE ARTICLE

ChemComm
www.rsc.org/chemcomm

Chemical synthesis of magnetic nanoparticles

Taeghwan Hyeon
National Creative Research Initiative Center for Oxide Nanocrystalline Materials and School of Chemical Engineering, Seoul National University, Seoul 151-744, Korea. E-mail: thyeon@plaza.snu.ac.kr

Received (in Cambridge, UK) 9th September 2002, Accepted 12th November 2002
First published as an Advance Article on the web 3rd December 2002

Recent advances in the synthesis of various magnetic nanoparticles using colloidal chemical approaches are reviewed. Typically, these approaches involve either rapid injection of reagents into hot surfactant solution followed by aging at high temperature, or the mixing of reagents at a low temperature and slow heating under controlled conditions. Spherical cobalt nanoparticles with various crystal structures have been synthesized by thermally decomposing dicobalt octacarbonyl or by reducing cobalt salts. Nanoparticles of Fe–Pt and other related iron or cobalt containing alloys have been made by simultaneously reacting their constituent precursors. Many different ferrite nanoparticles have been synthesized by the thermal decomposition of organometallic precursors followed by oxidation or by low-temperature reactions inside reverse micelles. Rod-shaped iron nanoparticles have been synthesized from the oriented growth of spherical nanoparticles, and cobalt nanodisks were synthesized from the thermal decomposition of dicobalt octacarbonyl in the presence of a mixture of two surfactants.

Introduction

The development of uniform nanometer sized particles has been intensively pursued because of their technological and fundamental scientific importance.[1] These nanoparticulate materials often exhibit very interesting electrical, optical, magnetic, and chemical properties, which cannot be achieved by their bulk counterparts.[2] The synthesis of discrete magnetic nanoparticles with sizes ranging from 2 to 20 nm, is of significant importance, because of their applications in multi-terabit in^{-2} magnetic storage devices.[3] Such magnetic nanoparticles could also find applications in ferrofluids, magnetic refrigeration systems, contrast enhancement in magnetic resonance imaging, magnetic carriers for drug targeting and catalysis.[4] In the current article, I will discuss recent advances made in the synthesis of various magnetic nanoparticles using colloidal chemical synthetic procedures. A general review on the synthesis and understanding of nanostructured magnetic materials up to 1996 is given in the article by Leslie-Pelecky and Rieke.[5] The materials covered in the current article are colloidal systems composed of isolated particles with nanometer-sized dimensions that are stabilized by surfactant molecules and dispersed in solvent media. In the ideal case, these non-interacting systems derive their unique magnetic properties mostly from the reduced size of the isolated nanoparticles, and contributions from interparticle interactions are negligible. The surfactant coating on magnetic nanoparticles prevents clustering due to steric repulsion. Dynamic adsorption and desorption of surfactant molecules onto particle surfaces during synthesis enables reactive species to be added onto the growing particles. These nanoparticles can be dispersed in many organic solvents and can be retrieved as powder forms by removing the solvent.

The followings are several key issues of nanoparticle synthesis.

- Particle size distribution (uniformity): Can we synthesize monodisperse nanocrystals?
- Particle size control: Can we control the particle size of nanocrystals in a reproducible manner?
- Crystallinity and crystal structure: Can we obtain materials with satisfactory high crystallinity and the desired crystal structure?
- Shape-control: Can we synthesize non-spherical and anisotropic nanoparticles?
- Alignment: For device applications, we should also consider the alignment of nanoparticles on substrates.

In the present article, I am especially interested in the synthesis of monodisperse magnetic nanoparticles. Monodisperse nanoparticles are generally considered to be samples with standard deviations $\sigma \leqslant 5\%$ diameter for spherical particles. Often nanocrystals are referred to as well-defined crystalline materials, whereas nanoparticles is a term used more generally for particles with diameters of 2–50 nm with variable crystallinity.

Chemical methods have been widely used to produce nanostructured materials due to their straightforward nature and their potential to produce large quantities of the final product. Realizable particle sizes range in size from nanometers to micrometers, by controlling particle size during synthesis by using competition between nucleation and growth. There are several synthetic procedures for synthesizing monodisperse nanoparticles. It is well known that a short burst of nucleation followed by slow controlled growth is critical to produce monodisperse particles. The following describe two representa-

Taeghwan Hyeon received his B. S. (1987) and M. S. (1989) in Chemistry from Seoul National University, Seoul, Korea. He obtained his Ph.D. from the University of Illinois at Urbana-Champaign (1996) under the supervision of Professor Kenneth S. Suslick. After conducting postdoctoral research with Professor Wolfgang M. H. Sachtler at Northwestern University, he joined the faculty of the School of Chemical Engineering of Seoul National University in September 1997. He has received several awards including the T. S. Piper Award (University of Illinois, 1996), Korean Young Scientist Award (Korean Government, 2002), KCS–Wiley Young Chemist Award (Korean Chemical Society, 2001), and The Scientist of the Month Award (Korean Science and Engineering Foundation, 2002). In July 2002, he became the director of the National Creative Research Initiative Center for Oxide Nanocrystalline Materials supported by the Korean Ministry of Science and Technology. His current research interests include synthesis of metallic and oxide nanoparticles, synthesis of nanoporous carbon materials, and catalytic applications of nanostructured materials.

DOI: 10.1039/b207789b

tive synthetic procedures. In the first synthetic procedure (Fig. 1), the rapid injection of the reagents, often organometallic

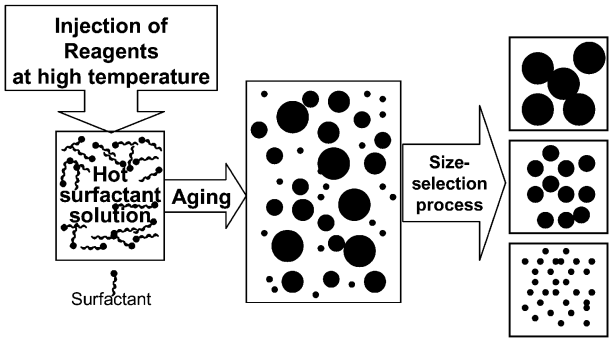

Fig. 1 Generalized synthesis of monodisperse nanoparticles by the injection of reagents into hot surfactant solution followed by aging and size-selective process.

compounds, into hot surfactant solution induces the simultaneous formation of many nuclei.[6] Alternatively, reducing agents are added to metal salt solutions at high temperature. In the second procedure, reagents are mixed at low temperature and the resulting reaction mixtures are slowly heated in a controlled manner to generate nuclei. Subsequently, particle growth occurs by the addition of reactive species. Particle size can be also increased by aging at high temperature by Oswalt ripening, in which smaller nanoparticles dissolve and deposit on the bigger nanoparticles. The growth of nanoparticles can be stopped by rapidly decreasing the reaction temperature. Nanoparticles produced using these synthetic procedures often have particle size distributions with $\sigma \sim 10\%$. Further size-selection processes can narrow the particle size distribution below $\sigma = 5\%$. The most frequently applied size-selection involves the addition of a poor solvent to precipitate the larger particles. When poor solvent is added to a mixture containing nanoparticles of various sizes, the biggest particles flocculate first because of their greatest van der Waals attraction. This precipitate can be retrieved by centrifugation. The precipitate can be re-dissolved in solvent, and further size-selection process can be performed to yield particles with narrower particle size distribution. Very recently, Klabunde and coworkers reported the fabrication of extremely monodisperse gold nanoparticles through digestive ripening.[7]

The particle sizes of nanoparticles can be controlled by systematically adjusting the reaction parameters, such as time, temperature, and the concentrations of reagents and stabilizing surfactants. In general, particle size increases with increasing reaction time, because more monomeric species are generated, and with increasing reaction temperature because the rate of reaction is increased.

Nanoparticles of iron, cobalt and nickel

The Murray group at the IBM Watson research center has studied the synthesis of monodisperse metallic magnetic nanoparticles intensively.[8,9] They have synthesized cobalt nanoparticles with several different crystal structures using different synthetic procedures. High temperature reduction of cobalt chloride was employed to synthesize ε-phase cobalt nanoparticles.[9a] The injection of superhydride ($LiBEt_3H$) solution in dioctyl ether into a hot cobalt chloride solution in dioctyl ether (200 °C) in the presence of oleic acid and trialkylphosphine induced the simultaneous formation of many small metal clusters, which acted as nuclei for nanoparticle formation. Continued heating at 200 °C induced the growth of these clusters to the nanoparticle level. Particle size was controlled by the steric bulkiness of the stabilizing surfactants. Short-chain alkylphosphines allowed faster growth, and resulted in the bigger particles, while bulkier surfactants reduced particle growth and favored production of smaller nanoparticles. For example, when bulky trioctylphosphine was applied in the synthesis, 2–6 nm sized particles were generated. In contrast, when tributylphosphine was used as a stabilizer 7–11 nm sized nanoparticles were produced. A further narrowing of particle size distribution was proceeded using a size selective precipitation by the gradual addition of alcohol (*e.g.* ethanol) into a hydrocarbon (*e.g.* hexane) dispersion containing nanoparticles with wide size distribution. Monodisperse cobalt nanoparticles organize into two- and three-dimensional superlattices. Fig. 2 shows a 2D assembly of 9 nm cobalt

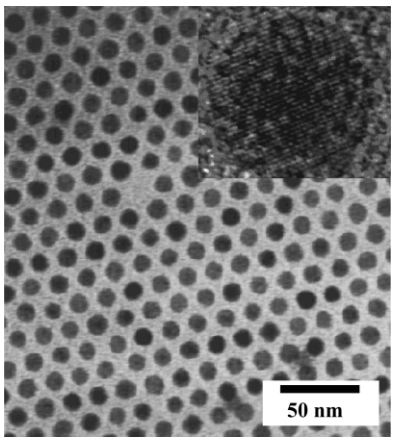

Fig. 2 TEM images of 9 nm ε-Co nanoparticles (inset, high-resolution TEM image).[9a] Reprinted with permission from reference 9(*a*). Copyright 1999 American Institute of Physics.

nanoparticles. A high-resolution transmission electron micrograph of a single nanoparticle, shown in the inset of Fig. 2, reveals its highly crystalline nature. The X-ray diffraction pattern of these nanoparticles reveals a complex cubic structure related to the beta phase of elemental manganese (ε-Co). Heating the ε-Co nanoparticles at 300 °C generated hcp Co nanoparticles. The Bawendi group have reported on the synthesis of ε-Co nanoparticle powders from the thermal decomposition of $Co_2(CO)_8$ in TOPO.[10] The Alivisatos group have reported on the synthesis of monodisperse ε-Co nanoparticles by the rapid pyrolysis of dicobalt octacarbonyl in the presence of a surfactant mixture composed of oleic acid, lauric acid and trioctylphosphine.[11] They could synthesize 3–17 nm sized cobalt nanoparticles by controlling the precursor/surfactant ratio, the reaction temperature, and the injection time. Black *et al.* later demonstrated spin-dependent electron transport using self-assembled 10 nm ε-Co nanoparticles over 100 nm wide electrodes.[12] Single electron tunneling was clearly observed for the two-dimensional hexagonal arrays of cobalt nanoparticles. Similar single electron tunneling in cobalt nanoparticles was also reported by Pileni and workers.[13]

Hcp cobalt nanoparticles were synthesized by using the so-called polyol process, in which high boiling alcohol is applied as both a reductant and a solvent.[8] In a typical synthesis, 1,2-dodecanediol is added into hydrated cobalt acetate solution dissolved in diphenyl ether containing oleic acid and trioctylphosphine at 250 °C. Nanoparticles were isolated by size-selective precipitation, and particle size was controlled by changing the relative concentration of precursor and stabilizer. For example, when a 1 : 1 molar ratio of cobalt acetate and oleic acid was used in the synthesis, 6–8 nm sized cobalt nanoparticles were produced, while increasing the concentration of stabilizing surfactants by a factor of two yielded smaller 3–6 nm nanoparticles. Particle size could be also varied by controlling the steric bulkiness of the phosphine stabilizers, for example,

using tributylphosphine, 10–13 nm Co nanoparticles were generated. Using hydrated nickel acetate as a metal precursor, nickel nanoparticles with particle sizes in the range 8–13 nm were obtained. Co/Ni alloy nanoparticles were also produced using a mixture of cobalt acetate and nickel acetate through a similar synthetic procedure.[8b] Diehl *et al.* used ferromagnetic resonance (FMR) techniques to investigate the detailed magnetic characteristics of cobalt nanoparticles with different crystalline structures.[9b] The structural characterization of an ordered assembly of cobalt nanoparticles using high-resolution transmission electron microscopy was reported by Wang *et al.*[9c] They synthesized multiply twinned fcc cobalt nanocrystals from the thermal decomposition of dicobalt octacarbonyl in the presence of a surfactant mixture composed of oleic acid and tributylphosphine. An HRTEM image of the nanoparticles revealed complicated interference patterns.[8]

Reverse micelles, which are water-in-oil droplets stabilized by a monolayer of surfactant, have been applied as nanoscale reactors for the synthesis of various nanoparticles.[14] Chen *et al.* and later the Pileni group reported on the synthesis of relatively uniform cobalt nanoparticles by the reduction of cobalt salt inside reverse micelles.[15] Chen *et al.* synthesized cobalt nanoparticles with particle size in the range 1.8–4.4 nm by reducing $CoCl_2$ with $NaBH_4$ in reverse micelles formed using didodecyldimethylammonium bromide (DDAB). The Pileni group reported the synthesis of cobalt nanoparticles from the reaction between a micellar solution containing NaAOT (sodium bis(2-ethylhexyl)sulfosuccinate) and $Co(AOT)_2$, and $NaBH_4$ dissolved in NaAOT solution.[16] Collisions followed by exchange between micellar droplets induce chemical reaction of cobalt ions and sodium borohydride to generate cobalt nanoparticles. The as-synthesized nanoparticles were poorly crystalline while XRD, after heating at 500 °C, revealed the characteristic pattern of fcc cobalt. The average particle size measured using TEM data was 6 nm with a particle size distribution σ = 9%. A size selection process involving the extraction of nanoparticles from reverse micelles significantly reduced the polydispersity of the particle size distribution and these uniform particles self-assembled to generate two-dimensionally hexagonally ordered arrays.[17]

Relatively very little work has been done to synthesize uniform iron nanoparticles. Suslick *et al.* reported the synthesis of iron nanoparticles from the sonochemical decomposition of iron pentacarbonyl in the presence of polyvinylpyrrolidone (PVP) or oleic acid.[18] The sonochemical decomposition of volatile organometallic compounds has been applied to synthesize various nanostructured materials.[19] Transmission electron micrographs showed that the iron particles ranged in size from 3 to 8 nm. Electron diffraction revealed that the particles as-formed are amorphous, and that after *in situ* electron beam heating they crystallized to bcc iron. These iron nanoparticles were readily oxidized to FeO when exposed to air. Gedanken and coworkers reported the synthesis of amorphous cobalt nanoparticles by sonicating $Co(CO)_3(NO)$ in decane solution in the presence of oleic acid.[20] Spherical 5–10 nm sized amorphous nanoparticles were produced. One drawback of the sonochemical process in the synthesis of nanoparticles is its inability to control particle size.

Very recently, our research group synthesized monodisperse iron nanoparticles from the high temperature (300 °C) aging of an iron–oleic acid metal complex, which was prepared by the thermal decomposition of iron pentacarbonyl in the presence of oleic acid at 100 °C.[21] We were able to synthesize monodisperse nanoparticles with sizes ranging from 4 to 20 nm without using any size selection process. Initially, the iron oleate complex was prepared by reacting $Fe(CO)_5$ and oleic acid at 100 °C. Iron nanoparticles were then generated by aging the iron complex at 300 °C. A TEM image of the iron nanoparticles revealed that the nanoparticles were monodisperse and the electron diffraction pattern showed that the nanoparticles were nearly amorphous. The XRD pattern of the sample after being heat-treated in an argon atmosphere at 500 °C revealed a bcc α-iron structure. The particle size could be controlled from 4 to 11 nm by using different molar ratios of iron pentacarbonyl to oleic acid. Fig. 3(a) and (b) show TEM images of iron nanoparticles with

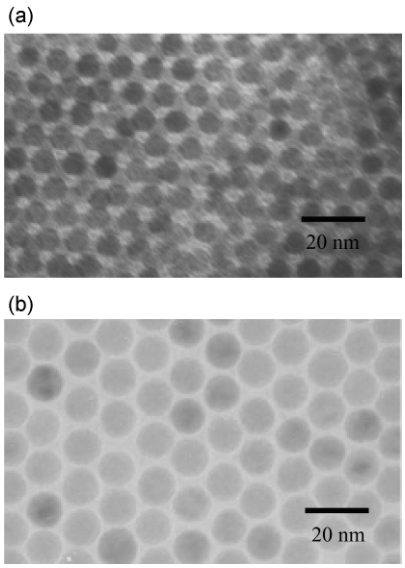

Fig. 3 TEM images of iron nanoparticles: (a) three-dimensional array of 7 nm Fe nanoparticles and (b) 11 nm Fe nanoparticles.

particle sizes of 7 and 11 nm, respectively, which were prepared using 1 : 2 and 1 : 3 molar ratios of $Fe(CO)_5$: oleic acid. In order to produce nanoparticles larger than 11 nm, a reaction mixture with a 1 : 4 molar ratio of $Fe(CO)_5$ and oleic acid was used during the synthesis. However, the particle size of the resulting nanoparticles was still around 11 nm. We could produce iron nanoparticles with particle sizes bigger than 11 nm by adding more iron oleate complex to previously prepared 11 nm iron nanoparticles, and then aging at 300 °C. Using this synthetic procedure, we were able to tune the particle sizes of the nanoparticles from 11 to 20 nm.

Using a similar synthetic procedure, we prepared moderately monodisperse cobalt nanoparticles and successfully applied them to recyclable catalysts for Pauson–Khand reactions, which involve the cycloaddition of alkynes, alkenes and carbon monoxide to synthesize cyclopentenones.[22] We also used aqueous colloidal cobalt nanoparticles stabilized by sodium dodecyl sulfate, which were synthesized by the reverse micelle method described above, for use as recyclable aqueous-phase Pauson–Khand catalysts.[23]

Nanoparticles of alloys of cobalt and iron

Sun *et al.* synthesized monodisperse iron–platinum nanoparticles by the simultaneous reduction of platinum acetylacetonate ($Pt(acac)_2$) and the thermal decomposition of iron pentacarbonyl ($Fe(CO)_5$) in the presence of oleic acid and oleyl amine.[24a] The composition was adjusted by changing the molar ratio of the two precursors. Using a 3 : 2 molar ratio of $Fe(CO)_5$ to $Pt(acac)_2$, $Fe_{48}Pt_{52}$ nanoparticles were produced, while using 4 : 1 mixtures $Fe_{70}Pt_{30}$ nanoparticles were formed. The particle size could be varied from 3 to 10 nm by adding more precursors to previously synthesized 3 nm particles, which acted as nuclei. When the solvent was evaporated slowly, three-dimensional superlattices are generated, and by controlling the chain lengths of the stabilizing surfactants, inter-particle spacing could be tuned. For example, 6 nm $Fe_{48}Pt_{52}$ nanoparticles were arranged

with an interparticle spacing of 4 nm using oleic acid and oleyl amine as stabilizers, while the same sized particles stabilized with hexanoic acid and hexyl amine exhibited ~1 nm spacing. Fig. 4 shows the TEM images of 6 nm sized $Fe_{50}Pt_{50}$

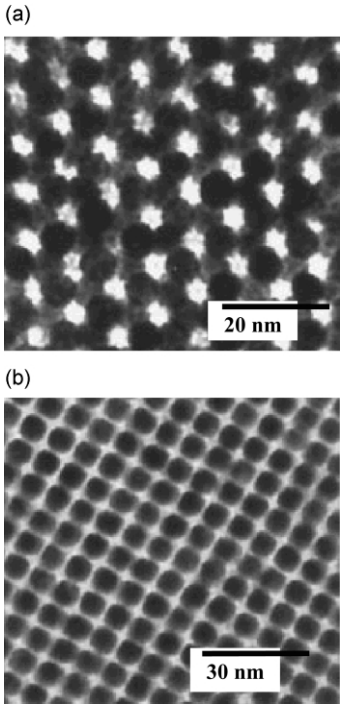

Fig. 4 TEM images of 6 nm sized $Fe_{50}Pt_{50}$ nanoparticles stabilized with oleic groups (a) and hexanoic groups (b).[24a] Reprinted with permission from reference 24(*a*). Copyright 2000 American Association for the Advancement of Science.

nanoparticles stabilized with oleic groups (Fig. 4(a)) and hexanoic groups (Fig. 4(b)), respectively. XRD analysis revealed that the as-synthesized nanoparticles showed a disordered face centered cubic (fcc) crystal structure and that this was transformed to an ordered face centered tetragonal structure when heated at 500 °C. Magnetic studies on 4 nm sized $Fe_{52}Pt_{48}$ nanoparticles showed that the as-synthesized nanoparticles were superparamagnetic at room temperature and that they became ferromagnetic after heating at 500 °C. A write/read experiment demonstrated that the annealed 120 nm thick superlattice of 4 nm $Fe_{48}Pt_{52}$ nanoparticles supported magnetization reversal transitions at moderate linear densities. Dai *et al.* reported the detailed structural characterization of Fe–Pt nanoparticles during annealing using high-resolution transmission electron microscopy.[24b] Very recently, Rogach and coworkers grew micrometer-sized colloidal crystals of Fe–Pt nanoparticles using a three-layer technique based on the slow diffusion of a non-solvent into a concentrated solution of nanoparticles.[25]

Using a similar synthetic procedure, Chen and Nikles reported the synthesis of FePd and CoPt nanoparticles.[26] 7 nm sized $Co_{48}Pt_{52}$ nanoparticles were synthesized by the simultaneous reduction of platinum acetylacetonate and the thermal decomposition of cobalt tricarbonylnitrosyl ($Co(CO)_3(NO)$) in the presence of oleic acid and oleyl amine. 11 nm $Fe_{50}Pd_{50}$ nanoparticles were produced using a similar synthetic method employing palladium acetylacetonate and iron pentacarbonyl as precursors. They also synthesized $Fe_xCo_yPt_{100-x-y}$ nanoparticles from the simultaneous reduction of cobalt acetylacetonate and platinum acetylacetonate and the thermal decomposition of iron pentacarbonyl in the presence of oleic acid and oleyl amine.[27] The average particle diameter was 3.5 nm and the particle size distribution was very narrow. Moreover, these nanoparticles self-assemble to generate superlattices, and when annealed the nanoparticles were transformed to the tetragonal phase.

Park and Cheon synthesized nanoparticles of Co–Pt alloys and $Co_{core}Pt_{shell}$ *via* transmetalation reactions.[28] The injection of 0.25 mmol of $Co_2(CO)_8$ into hot toluene solution containing 0.5 mmol of $Pt(hfac)_2$ and oleic acid produced $CoPt_3$ alloy nanoparticles with a particle size of 1.8 nm (σ = 0.1 nm). Reaction of $Pt(hfac)_2$ with previously prepared 6.33 nm sized Co nanoparticles produced moderately monodisperse $Co_{core}Pt_{shell}$ nanoparticles with a particle size of 6.27 nm (σ = 0.58 nm). The Pt shell thickness and the Co core size were estimated to be 1.82 and 4.75 nm, respectively.

Chaudret and coworkers reported the synthesis of 1–2 nm sized bimetallic Co–Pt nanoparticles from the reaction of $Co(\eta^3\text{-}C_8H_{13})(\eta^4\text{-}C_8H_{12})$ and $Pt_2(dba)_3$ (dba = dibenzylideneacetone) under dihydrogen.[29] The composition of the nanoparticles could be varied by changing the initial molar ratio of the two organometallic precursors. XRD and TEM analysis revealed that the Pt rich particles adopted a fcc crystalline structure while the cobalt rich particles adopted a polytetrahedral arrangement.

Nanoparticles of ferrites

Transition metal oxides constitute one of the most fascinating classes of inorganic solids, as they exhibit a very wide variety of structures, properties, and phenomena.[30] Oxide materials have been employed in many important advanced technology areas due to their many interesting physical properties, including magnetic, ferroelectric, superconducting, ionic and electrical conducting characteristics. Nanoparticles of magnetic oxides, including most representative ferrites, have been studied for many years for their applications as magnetic storage media and as ferrofluids. However, the synthesis of monodisperse magnetic oxide nanoparticles was only reported very recently.

The Alivisatos group reported the synthesis of γ-Fe_2O_3 nanoparticles from the thermal decomposition of iron Cupferron complexes (Cup: *N*-nitrosophenylhydroxylamine, $C_6H_5N(NO)O^-$).[31] Particle sizes were controlled by either varying the reaction temperature or by using a varying amount of the complex. Relatively uniform 4–10 nm sized γ-Fe_2O_3 nanoparticles were synthesized. Using different metal Cupferron complexes, nanoparticles of Mn_3O_4 and Cu_2O were also generated.

Very recently, our group reported on the synthesis of monodisperse and highly-crystalline maghemite nanoparticles, which did not involve a size selection process.[21] The overall synthetic procedure is depicted in the Fig. 5. Monodisperse iron nanoparticles were first synthesized, and then they were transformed to monodisperse γ-Fe_2O_3 nanocrystals by controlled oxidation using trimethylamine *N*-oxide ($(CH_3)_3NO$), as a mild oxidant. In the current synthetic process, the size uniformity was determined during the synthesis of metallic nanoparticles. Transmission electron microscopic images of the particles showed two- and three-dimensional assembly of particles, demonstrating the uniformity of these nanoparticles. Electron diffraction, X-ray diffraction, and high-resolution transmission electron microscopy proved the highly crystalline nature of the γ-Fe_2O_3 structures. XPS and Raman spectroscopic results confirmed the γ-Fe_2O_3 structures. Particle size could be varied from 4 to 20 nm by altering the experimental parameters. The dominating size controlling factor was the molar ratio of iron pentacarbonyl to oleic acid. Fig. 6(a) and (b) show the TEM images of maghemite nanoparticles with sizes of 7 and 11 nm that were synthesized by using reaction mixtures with [$Fe(CO)_5$]:[oleic acid] molar ratios of 1:2 and 1:3, respectively. As described in the synthesis of iron nanoparticles, nano-

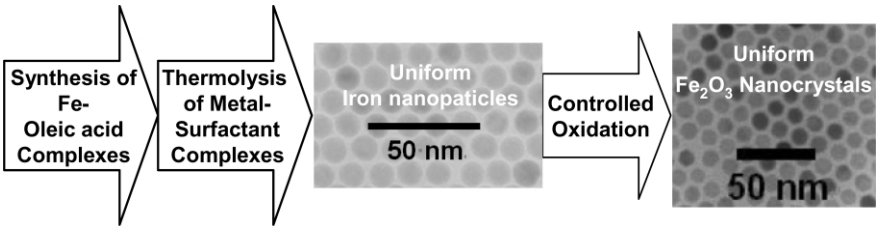

Fig. 5 Synthetic procedure for monodisperse γ-Fe_2O_3 nanoparticles.

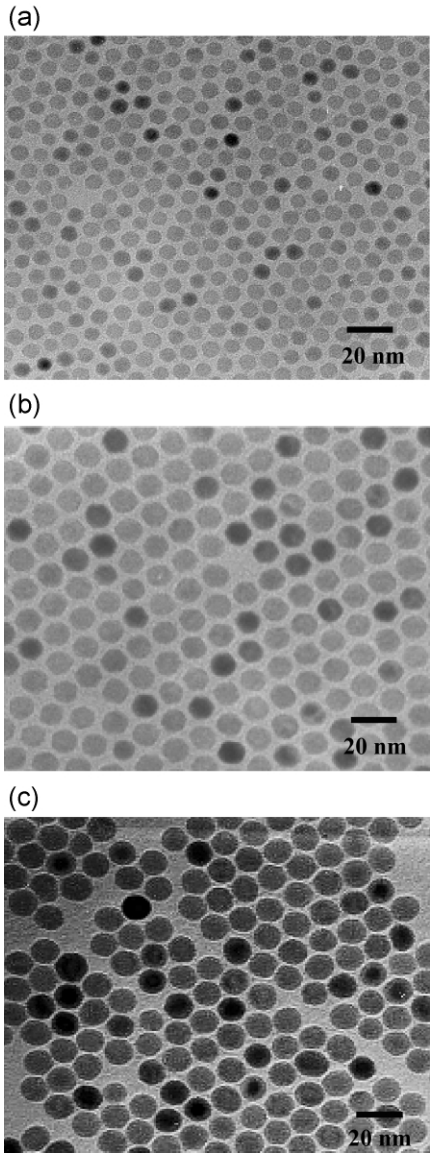

Fig. 6 TEM images of γ-Fe_2O_3 nanoparticles: (a) 7 nm, (b) 11 nm, (c) 13 nm.[21] Reprinted with permission from reference 21. Copyright 2001 American Chemical Society.

particles larger than 11 nm were synthesized by a seeded growth process, employing addition of more iron–oleate complex to the 11 nm sized particles followed by aging at 300 °C. The resulting larger iron nanoparticles were then transformed to iron oxide nanocrystals by oxidizing with trimethylamine *N*-oxide. We could also synthesize monodisperse γ-Fe_2O_3 nanocrystals by directly injecting $Fe(CO)_5$ into a solution containing both the surfactant and trimethylamine *N*-oxide. Fig. 6(c) shows a TEM image of 13 nm sized γ-Fe_2O_3 nanocrystals synthesized through the direct injection method. However, the first method employing the synthesis of monodisperse iron nanoparticles followed by mild oxidation allowed better control of particle size and reproducibility.

Using a similar procedure, based on the thermal decomposition of a metal–surfactant complex followed by mild oxidation, we synthesized highly crystalline and monodisperse cobalt ferrite ($CoFe_2O_4$) nanocrystals.[32] In this synthesis, uniform iron–cobalt alloy nanoparticles were first generated from the thermal decomposition of a metal–oleate complex, and then further oxidized to yield cobalt ferrite nanocrystals. A single molecular precursor, (η^5-C_5H_5)$CoFe_2(CO)_9$, was employed in the synthesis of the mixed-metal–oleate complex. The as-synthesized poorly crystalline metallic nanoparticles were then transformed into cobalt ferrite nanocrystals by oxidizing them with the mild oxidant, trimethylamine *N*-oxide. Cobalt ferrite nanoparticles with particle diameters of 6 nm were synthesized using starting reaction mixtures with a metal precursor to oleic acid molar ratio of 1 : 3. The uniformity of the nanocrystals was further demonstrated by the formation of a three-dimensional close-packed superlattice assembly. Larger 9 nm sized nanocrystals, as shown in Fig. 7, were produced when lauric acid was

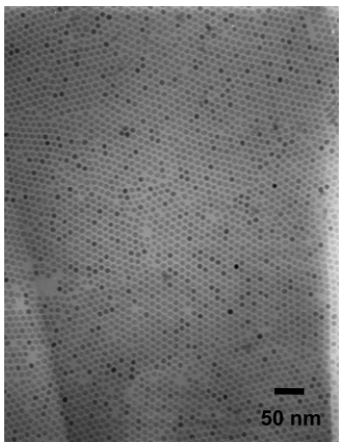

Fig. 7 TEM images of 9 nm sized cobalt ferrite nanoparticles.[32] Reprinted with permission from reference 32. Copyright 2002 American Chemical Society.

used in combination with oleic acid at a molar ratio of [metal precursor] : [oleic acid] : [lauric acid] = 1 : 1 : 2. Monodisperse nanocrystals were obtained without a further size selection process. Nanoscale elemental analysis of ten 9 nm cobalt ferrite nanocrystals by energy-dispersive X-ray spectroscopy (EDS) showed that an average molar atomic ratio of Fe to Co was 2.3 with a standard deviation of 20%. The EDS data well matched the bulk elemental analysis results obtained by inductively coupled plasma atomic emission spectrometry (ICP-AES).

Moumen and Pileni reported on a synthesis of cobalt ferrite nanoparticles using a microemulsion method,[33] which had been introduced earlier by Klabunde and coworkers.[34] Aqueous methylamine (CH_3NH_3OH) was added to sodium dodecyl sulfate solution containing cobalt(II) dodecyl sulfate ($Co(DS)_2$) and iron(II) dodecyl sulfate ($Fe(DS)_2$) to generate a precipitate. The size of the nanoparticles was controlled from 2 to 5 nm by changing the sodium dodecyl sulfate concentration and by

maintaining constant concentrations of $Co(DS)_2$, $Fe(DS)_2$, and methylamine. The particles were not well-isolated and aggregated into networks, and the particle size was not uniform with a standard deviation of about 30%. Later, detailed structural and magnetic characterizations of these cobalt ferrite nanoparticles were reported by Zhang and coworkers.[35] From neutron diffraction studies, they calculated that 78% of tetrahedral sites (the A site in normal spinel structure with the general formula of AB_2O_4) were occupied by Fe^{3+} cations. The 12 nm nanoparticles had a blocking temperature of 320 K. The same research group also prepared magnesium ferrite nanoparticles using a similar microemulsion method, and the magnetic properties were compared with cobalt ferrite nanoparticles.[36] The blocking temperature of cobalt ferrite was found to be at least 150 K higher than that of the same sized magnesium ferrite nanoparticles.

Markovich and coworkers synthesized magnetite (Fe_3O_4) nanoparticles by reacting aqueous ammonia with an aqueous solution containing $FeCl_3$ and $FeCl_2$ at a molar ratio of 2 : 1.[37] The aqueous nanoparticles were dispersible in hexane after being coated with oleic acid. After several cycles of size-selective precipitation, uniform nanoparticles were obtained. The Langmuir–Blodgett (LB) technique was used to produce two-dimensional (2D) arrays of these uniform nanoparticles.

Very recently, Sun and Zeng synthesized monodisperse magnetite nanoparticles from a high temperature reaction of iron(III) acetylacetonate ($Fe(acac)_3$).[38] For example, 4 nm sized magnetite nanoparticles were synthesized by refluxing a reaction mixture composed of 2 mmol of $Fe(acac)_3$, 20 mL of diphenyl ether, 10 mmol of 1,2-hexadecanediol, 6 mmol of oleic acid, and 6 mmol of oleyl amine. A seed-mediated growth method was used to synthesize larger nanoparticles. Smaller sized nanoparticles (< 4 nm) were mixed with more precursor materials and the resulting mixture was refluxed to produce the larger nanoparticles. By controlling the quantity of the nanoparticle seeds, various sized larger nanoparticles were generated. Fig. 8 shows the TEM image of 16 nm Fe_3O_4 nanoparticles. The as-synthesized magnetite nanoparticles were transformed to either maghemite (γ-Fe_2O_3) or iron (α-Fe) by annealing in an oxygen or in an argon atmosphere, respectively.

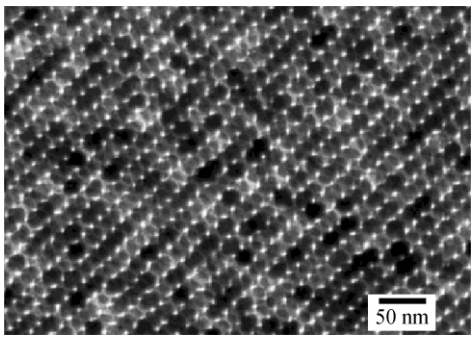

Fig. 8 TEM images of three-dimensional array of 16 nm Fe_3O_4 nanoparticles.[38] Reprinted with permission from reference 38. Copyright 2002 American Chemical Society.

Shape control of nanoparticles

Recently, the shape control of nanoparticles to generate anisotropic nanoparticles was recognized as a very important issue. The Alivisatos group reported the synthesis of rod-shaped CdSe nanocrystals from the high temperature reaction between dimethylcadmium and selenium in the presence of a mixed surfactant solution composed of trioctylphosphine oxide and hexylphosphonic acid.[39] Later the same group reported on the synthesis of rod-, arrow-, teardrop- and tetrapod-shaped CdSe nanocrystals by controlling experimental conditions such as the ratio of surfactants, the injection volume, and the time-dependent monomer concentration.[40] They explained the formation of anisotropic rod-shaped nanoparticles based on the relative differences between the growth rates of different crystal faces at high monomer concentration. Cheon and coworkers described the synthesis of CdS nanorods and of related nanostructures in pure hexadecylamine using a single-source molecular precursor, $Cd(S_2CNEt_2)_2$.[41] The Peng group conducted detailed mechanistic studies on the shape-controlled synthesis of CdSe nanoparticles, and explained the growth of anisotropic CdSe nanocrystals on the basis of diffusion control.[42] Wang and coworkers synthesized gold nanorods using an electrochemical method.[43] In this synthesis, the electrochemical cell consisted of a gold anode and platinum cathode and the electrolyte solution was a solution of hexadecyltrimethylammonium bromide and tetradecylammonium bromide. The aspect ratios of the nanorods were controlled by surfactant molar ratios.

Anisotropic magnetic nanoparticles are expected to offer many advantages because shape anisotropy would exert a tremendous influence on their magnetic properties. The tendency for the magnetization to align in a particular direction in a specimen is denoted magnetic anisotropy. Magnetic anisotropy generally originates from crystal symmetry, shape, stress, or directed atomic pair ordering.[3d,5,44] Of these, crystalline anisotropy and shape anisotropy are common forms of anisotropy in magnetic materials. Symmetrically shaped nanoparticles, such as spheres, do not have any net shape anisotropy. However, rod-shaped nanoparticles have shape anisotropy in addition to crystalline anisotropy, which will increase the coercivity. Submicrometer-sized acicular (rod-shaped) magnetic particles have been used in commercial particulate magnetic recording media.

Relatively few anisotropic magnetic nanoparticles have been reported until 2000. Particle dimensions of the anisotropic magnetic nanoparticles are too big to exhibit any nanosize effect and these materials were often extensively agglomerated.[45] Gibson and Putzer reported on the synthesis of disk-shaped cobalt nanoparticles of width 100 nm and thickness 15 nm by sonicating an aqueous solution of Co^{2+} and hydrazine.[45] The nanoparticles obtained were single-domain particles. The particles were not uniform and agglomerated.

Our group reported the synthesis of nearly uniform rod-shaped iron nanoparticles from the controlled growth of monodisperse spherical nanoparticles.[46] In the first step of the synthesis, monodisperse 2 nm spherical iron nanoparticles were prepared by the thermal decomposition of an organometallic precursor ($Fe(CO)_5$) in the presence of a stabilizing surfactant, trioctylphosphine oxide (TOPO). An aliquot of $Fe(CO)_5$ in trioctylphosphine (TOP) was added to the resulting spherical nanoparticles in TOPO, at 320 °C, and the resulting black solution was aged for 30 min at 320 °C. The nanoparticles so produced were retrieved by precipitation. The precipitate was dissolved in 19 mL of pyridine containing 0.5 g of didodecyldimethylammonium bromide (DDAB), and the resulting solution was refluxed for 12 h. The precipitate formed during the reflux was removed by centrifugation and the supernatant was vacuum-dried to yield a black powder. A TEM image of the sample (Fig. 9) revealed nearly monodisperse rod-shaped particles of dimensions 2 nm (width) $\times$ 11 nm (length) with a standard deviation of 5.7% in the length. The electron diffraction pattern showed the bcc structure of α-Fe. When the DDAB concentration in pyridine was increased, rod-shaped particles with higher aspect ratios were obtained. The width of these nanorods (2 nm) was almost unchanged, but the length increased to 22 nm (standard deviation of 5.9%) and 27 nm (standard deviation of 5.5%). The transformation of nano-

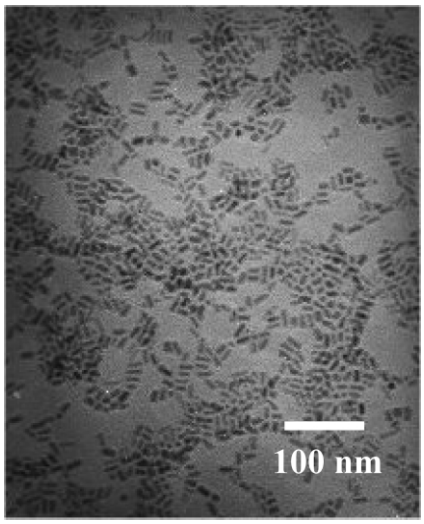

Fig. 9 TEM images of rod-shaped 2 nm (width) × 11 nm (length) iron nanoparticles.[46] Reprinted with permission from reference 46. Copyright 2000 American Chemical Society.

spheres to nanorods seems to be due to the so-called oriented attachment mechanism, which is initiated by the relatively strong binding of DDAB surfactant on the central region of the growing nanoparticles. After the fusion of two nanospheres, a third nanosphere will bind on the edge (instead of the central region where the DDAB is strongly bound), thus generating a catenated structure. The continued attachment of nanospheres onto the ends of the growing nanoparticles generates the unidirectional nanorods. In some parts of TEM image, catenated nanospheres, which seem to be of the intermediate structure, were observed. Magnetic studies revealed that the blocking temperatures of 2 nm × 11 nm rod-shaped nanoparticles and 2 nm spherical nanoparticles were 110 and 12 K, respectively. These results are consistent with classical micromagnetic theory, which predicts that the anisotropy energy is proportional to the volume of a single particle and the anisotropy constant. The magnetic anisotropy constant (K) was deduced from the blocking temperature using the equation $K = 25k_bT_B/V$, where k_b is the Boltzman constant and V is the volume of single nanoparticle.[47] The magnetic anisotropy constant of 2 nm nanospheres was calculated to be 9.1×10^6 erg cm^{-3}, and that of the rod-shaped particles as 1.6×10^7 erg cm^{-3}. By treating the rod-shaped particles as prolate spheroids, the shape anisotropy constant of 2 nm × 11 nm rod-shaped nanoparticles was calculated to be 7.9×10^6 erg cm^{-3}. When this shape anisotropy constant was added to the magnetocrystalline anisotropy constant of the spheres, the overall value was found to agree well with the experimentally determined anisotropy constant of the rod-shaped particles.[48] The longer iron nanorods with lengths of 22 nm, 27 nm, and 37 nm were found to be readily oxidized to FeO.

The Alivisatos group extended the synthetic procedure developed for CdSe nanorods to synthesize cobalt nanorods,[49a] which are now confirmed to be nanodisks as will be discussed below.[49b] In this synthesis, dicobalt octacarbonyl, $Co_2(CO)_8$, in *o*-dichlorobenzene was injected into hot (185 °C) *o*-dichlorobenzene solution containing oleic acid and trioctylphosphine oxide (TOPO). Quenching of the reaction mixture shortly after this injection then generated relatively uniform sized cobalt nanorods (nanodisks) with a hcp crystal structure. Upon further thermal aging of several minutes, the high-energy hcp rod (disk)-shaped particles were transformed to monodisperse spherical ε-Co nanocrystals. The change of crystal structure at the relatively low temperature of < 200 °C can be explained by the facile diffusion and phase transitions for nanometer sized particles. The transformation to spherical particles was explained by the high surface tension that reduces the surface-to-volume ratio. The size of nanoparticles could be controlled by the ratio of surfactant to precursor, which is consistent with observations in the synthesis of CdSe and other nanoparticles. The use of two different surfactants seemed to be important for the synthesis of disk-shaped nanoparticles by modulating the relative growth rates of different faces. At a fixed oleic acid concentration, the length of the nanorods (nanodisks) was found to be proportional to the concentration of TOPO. High resolution transmission electron microscopic images showed that the long direction of the nanorods (nanodisks) is parallel to the (101) planes, demonstrating that TOPO selectively stabilizes the (101) face of Co and decreases its relative growth rate. The size uniformity was demonstrated by the spontaneous self-assembly of the nanocrystals and by the formation of superstructures such as ribbons of nanorods (nanodisks). A TEM image of self-assembled 4 nm by 25 nm hcp Co nanorods (nanodisks) is shown in Fig. 10.

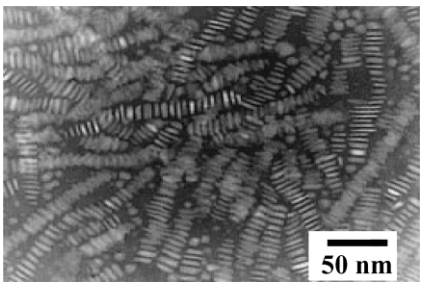

Fig. 10 TEM images of 4 nm (width) × 25 nm (length) disk-shaped cobalt nanoparticles.[49a] Reprinted with permission from reference 49(*a*). Copyright 2001 American Association for the Advancement of Science.

Very recently, the same research group reported the synthesis of hcp-Co nanodisks, which were thought to be nanorods as described above.[49b] The disk-shape of the nanocrystals was verified by tilting experiments in TEM. The same workers developed a much easier procedure to synthesize cobalt nanodisks, employing a linear amine instead of TOPO. Thermal decomposition of dicobalt octacarbonyl in the presence of oleic acid and a linear amine followed by aging generated disk-shaped nanoparticles along with spherical nanoparticles. A pure fraction of hcp Co nanodisks could be obtained after magnetic separation. The length and diameter can be controlled, primarily by variation of the reaction time following nucleation as well as by varying the precursor to surfactant ratios. The average size of the smaller disks was about 2 × 4 nm and about 4 × 90 nm for the largest.

Chaudret and coworkers reported on the synthesis of nickel nanorods from the reduction of $Ni(COD)_2$ (COD = cycloocta-1,5-diene) in the presence of hexadecylamine.[50] They reported that increasing concentrations of amine induced the formation of nanorods. Magnetic studies revealed that these nanorods showed a saturation magnetization close to the bulk value, demonstrating the absence of the influence of amine coordination on magnetic properties of the nanorods. Gedanken and coworkers reported the fabrication of the magnetite nanorods by the sonication of aqueous iron(II) acetate in the presence of β-cyclodextrin.[51]

Conclusion and outlook

In the past few years, considerable progress has been made in the synthesis of monodisperse and well-defined structured magnetic nanoparticles with sizes ranging from 2 to 20 nm. The outlook of such magnetic nanoparticles is very promising because these materials will find many important industrial applications including ultrahigh-density magnetic storage

media and drug-delivery systems. From a synthetic point of view, there are several interesting research areas worth pursuing. First, we need a generalized synthetic procedure, which can synthesize various monodisperse nanoparticles directly without any further size-selection process. Second, magnetic nanoparticles with various chemical compositions, such as CrO_2 and lanthanide-containing materials, should be prepared. Third, more extensive shape-control of magnetic nanoparticles should be investigated. Forth, a large-area alignment of magnetic nanoparticles is critical in magnetic storage media applications. To improve our understanding of such systems and their applications, a collaborative multi-disciplined effort is anticipated.

Acknowledgements

The work was supported by the National Creative Research Initiative Program of the Korean Ministry of Science and Technology. I thank my students, Dr Sang-Wook Kim, Jongnam Park, Sang-Jae Park and Yunhee Chung for their important contributions to the work discussed herein. I also thank Dr Shouheng Sun and Dr Chris Murray at IBM T. J. Watson Research Center for very helpful discussion on Fe–Pt alloy nanoparticles.

Notes and references

1 (*a*) A. P. Alivisatos, *Science*, 1996, **271**, 933; (*b*) H. Weller, *Angew. Chem., Int. Ed. Engl.*, 1993, **32**, 41; (*c*) *Clusters and Colloids*, ed. G. Schmid, VCH Press, New York, 1994; (*d*) *Nanoscale Materials in Chemistry*, ed. K. J. Klabunde, Wiley-Interscience, New York, 2001; (*e*) *Nanoparticles and Nanostructured Films*, ed. J. H. Fendler, Wiley-VCH, Weinheim, 1998.

2 (*a*) S. A. Majetich and Y. Jin, *Science*, 1999, **284**, 470; (*b*) C. B. Murray, C. R. Kagan and M. G. Bawendi, *Science*, 1995, **270**, 1335; (*c*) A. J. Zarur and J. Y. Ying, *Nature*, 2000, **403**, 65.

3 (*a*) D. D. Awschalom and D. P. DiVicenzo, *Phys. Today*, 1995, **4**, 43; (*b*) K. Raj and R. Moskowitz, *J. Magn. Magn. Mater.*, 1990, **85**, 233; (*c*) I. M. L. Billas, A. Chatelain and W. A. de Heer, *Science*, 1994, **265**, 1682; (*d*) R. C. O'Handley, *Modern Magnetic Materials*, Wiley, New York, 1999.

4 (*a*) V. E. Fertman, *Magnetic Fluids Guidebook: Properties and Applications*, Hemisphere Publishing Co., New York, 1990; (*b*) B. M. Berkovsky, V. F. Medvedev and M. S. Krakov, *Magnetic Fluids: Engineering Applications*, Oxford University Press, Oxford, 1993; (*c*) R. F. Ziolo, E. P. Giannelis, B. A. Weinstein, M. P. O'Horo, B. N. Ganguly, V. Mehrotra, M. W. Russel and D. R. Huffman, *Science*, 1992, **257**, 219.

5 D. L. Leslie-Pelecky and R. D. Rieke, *Chem. Mater.*, 1996, **8**, 1770.

6 C. B. Murray, D. J. Norris and M. G. Bawendi, *J. Am. Chem. Soc.*, 1993, **115**, 8706.

7 (*a*) X. M. Lin, H. M. Jaeger, C. M. Sorensen and K. J. Klabunde, *J. Phys. Chem. B*, 2001, **105**, 3353; (*b*) S. Stoeva, K. J. Klabunde, C. M. Sorensen and I. Dragieva, *J. Am. Chem. Soc.*, 2002, **124**, 2305.

8 (*a*) C. B. Murray, S. Sun, W. Gaschler, H. Doyle, T. A. Betley and C. R. Kagan, *IBM J. Res. & Dev.*, 2001, **45**, 47; (*b*) C. B. Murray, S. Sun, H. Doyle and T. A. Betley, *MRS Bull.*, 2001, 985.

9 (*a*) S. Sun and C. B. Murray, *J. Appl. Phys.*, 1999, **85**, 4325; (*b*) M. R. Diehl, J.-Y. Yu, J. R. Heath, G. A. Held, H. Doyle, S. Sun and C. B. Murray, *J. Phys. Chem. B*, 2001, **105**, 7913; (*c*) Z. L. Wang, Z. Dai and S. Sun, *Adv. Mater.*, 2000, **12**, 1944.

10 D. P. Dinega and M. G. Bawendi, *Angew. Chem., Int. Ed.*, 1999, **38**, 1788.

11 V. F. Puntes, K. M. Krishnan and A. P. Alivisatos, *Appl. Phys. Lett.*, 2001, **78**, 2187.

12 C. T. Black, C. B. Murray, R. L. Sandstrom and S. Sun, *Science*, 2000, **290**, 1131.

13 C. Petit, T. Cren, D. Roditchev, W. Sacks, J. Klein and M. P. Pileni, *Adv. Mater.*, 1999, **11**, 1198.

14 M. P. Pileni, *Langmuir*, 1997, **13**, 3266.

15 J. P. Chen, C. M. Sorensen, K. J. Klabunde and G. C. Hadjipanayis, *J. Appl. Phys.*, 1994, **76**, 6316.

16 C. Petit, A. Taleb and M. P. Pileni, *J. Phys. Chem. B*, 1999, **103**, 1805.

17 C. Petit, A. Taleb and M. P. Pileni, *Adv. Mater.*, 1998, **10**, 259.

18 K. S. Suslick, M. Fang and T. Hyeon, *J. Am. Chem. Soc.*, 1996, **118**, 11960.

19 K. S. Suslick, T. Hyeon and M. Fang, *Chem. Mater.*, 1996, **8**, 2172.

20 K. V. P. M. Shafi, A. Gedanken and R. Prozorov, *Adv. Mater.*, 1998, **10**, 590.

21 T. Hyeon, S. S. Lee, J. Park, Y. Chung and H. B. Na, *J. Am. Chem. Soc.*, 2001, **123**, 12798.

22 S.-W. Kim, S. U. Son, S. S. Lee, T. Hyeon and Y. K. Chung, *Chem. Commun.*, 2001, 2212.

23 S. U. Son, S. I. Lee, Y. K. Chung, S.-W. Kim and T. Hyeon, *Org. Lett.*, 2002, **4**, 277.

24 (*a*) S. Sun, C. B. Murray, D. Weller, L. Folks and A. Moser, *Science*, 2000, **287**, 1989; (*b*) Z. R. Dai., S. Sun and Z. L. Wang, *Surf. Sci.*, 2002, **505**, 325.

25 E. Shevchenko, D. Talapin, A. Kornowski, F. Wiehorst, J. Koetzler, M. Haase, A. Rogach and H. Weller, *Adv. Mater.*, 2002, **14**, 287.

26 M. Chen and D. E. Nikles, *J. Appl. Phys.*, 2002, **91**, 8477.

27 M. Chen and D. E. Nikles, *NanoLett.*, 2002, **2**, 211.

28 J.-I. Park and J. Cheon, *J. Am. Chem. Soc.*, 2001, **123**, 5743.

29 T. O. Ely, C. Pan, C. Amiens, B. Chaudret, F. Dassenoy, P. Lecante, M.-J. Casanove, A. Mosset, M. Respaud and J.-M. Broto, *J. Phys. Chem. B*, 2000, **104**, 695.

30 (*a*) C. N. R. Rao and B. Raveau, *Transition Metal Oxides*, Wiley-VCH, New York, 2nd edn., 1998; (*b*) R. M. Cornell and U. Schwertmann, *The iron oxides*, VCH, Weinheim, 1996.

31 J. Rockenberger, E. C. Scher and A. P. Alivisatos, *J. Am. Chem. Soc.*, 1999, **121**, 11595.

32 T. Hyeon, Y. Chung, J. Park, S. S. Lee, Y.-W. Kim and B. H. Park, *J. Phys. Chem. B*, 2002, **106**, 6831.

33 (*a*) N. Moumen and M. P. Pileni, *Chem. Mater.*, 1996, **8**, 1128; (*b*) N. Moumen and M. P. Pileni, *J. Phys. Chem.*, 1996, **100**, 1867.

34 J. P. Chen, K. M. Lee, C. M. Sorensen, K. J. Klabunde and G. C. Hadjipanayis, *J. Appl. Phys.*, 1994, **75**, 5876.

35 C. Liu, B. Zou, A. J. Rondinone and Z. J. Zhang, *J. Am. Chem. Soc.*, 2000, **122**, 6263.

36 A. J. Rondinone, A. C. S. Samia and Z. J. Zhang, *J. Phys. Chem.*, 1999, **103**, 6876.

37 T. Fried, G. Shemer and G. Markovich, *Adv. Mater.*, 2001, **13**, 1158.

38 S. Sun and H. Zeng, *J. Am. Chem. Soc.*, 2002, **124**, 8204.

39 X. Peng, L. Manna, W. Yang, J. Wickham, E. Scher, A. Kadavanich and A. P. Alivisatos, *Nature*, 2000, **404**, 59.

40 L. Manna, E. Scher and A. P. Alivisatos, *J. Am. Chem. Soc.*, 2000, **122**, 12700.

41 Y.-W. Jun, S.-M. Lee, N.-J. Kang and J. Cheon, *J. Am. Chem. Soc.*, 2001, **123**, 5150.

42 (*a*) Z. A. Peng and X. Peng, *J. Am. Chem. Soc.*, 2001, **123**, 1389; (*b*) Z. A. Peng and X. Peng, *J. Am. Chem. Soc.*, 2002, **124**, 3343.

43 (*a*) Y. Y. Yu, S. Chang, C. J. Lee and C. R. C. Wang, *J. Phys. Chem. B*, 1997, **101**, 6661; (*b*) S.-S. Chang, C.-W. Shih, C.-D. Chen, W.-C. Lai and C. R. C. Wang, *Langmuir*, 1999, **15**, 701; (*c*) S. Link, M. B. Mohamed and M. A. El-Sayed, *J. Phys. Chem. B*, 1999, **103**, 3073.

44 For the general introduction on the magnetic properties of anisotropic magnetic nanoparticles, please refer to ch. 6 (Magnetism) of ref. 1*c*.

45 C. P. Gibson and K. J. Putzer, *Science*, 1995, **267**, 1338.

46 S.-J. Park, S. Kim, S. Lee, Z. G. Khim, K. Char and T. Hyeon, *J. Am. Chem. Soc.*, 2000, **122**, 8581.

47 Q. Chen and Z. J. Zhang, *Appl. Phys. Lett.*, 1998, **73**, 3156.

48 B. D. Cullity, *Introduction to Magnetic Materials*, Addison-Wesley, Reading, MA, 1972.

49 (*a*) V. F. Puntes, K. M. Krishnan and A. P. Alivisatos, *Science*, 2001, **291**, 2115; (*b*) V. F. Puntes, D. Zanchet, C. K. Erdonmez and A. P. Alivisatos, *J. Am. Chem. Soc.*, 2002, **124**, 12874.

50 N. Cordente, M. Respaud, F. Senocq, J.-J. Casanove, C. Amiens and B. Chaudret, *NanoLett.*, 2001, **1**, 565.

51 R. V. Kumar, Y. Koltypin, X. N. Xu, Y. Yeshurun, A. Gedanken and I. Felner, *J. Appl. Phys.*, 2001, **89**, 6324.